Applied Catalysis B: Environmental 83 (2008) 202–207

Contents lists available at ScienceDirect

Applied Catalysis B: Environmental

journal homepage: www.elsevier.com/locate/apcatb

Efficient decomposition of organic compounds with $FeTiO_3/TiO_2$ heterojunction under visible light irradiation

Bifen Gao, Yong Joo Kim, Ashok Kumar Chakraborty, Wan In Lee *

Department of Chemistry, Inha University, Incheon 402-751, Republic of Korea

ARTICLE INFO

Article history:
Received 16 August 2007
Received in revised form 13 February 2008
Accepted 16 February 2008
Available online 26 February 2008

Keywords:
Photocatalyst
Visible light
$FeTiO_3$
TiO_2
$FeTiO_3/TiO_2$
Heterojunction
Decomposition
CO_2 evolution

ABSTRACT

$FeTiO_3/TiO_2$, a new heterojunction-type photocatalyst working at visible light, was prepared by a simple sol–gel method. Not only did $FeTiO_3/TiO_2$ exhibit greatly enhanced photocatalytic activity in decomposing 2-propanol in gas phase and 4-chlorophenol in aqueous solution, but also it induced efficient mineralization of 2-propanol under visible light irradiation ($\lambda \geq 420$ nm). Furthermore, it showed a good photochemical stability in repeated photocatalytic applications. $FeTiO_3$ showed a profound absorption over the entire visible range, and its valence band (VB) position is close to that of TiO_2. The unusually high photocatalytic efficiency of the $FeTiO_3/TiO_2$ composite was therefore deduced to be caused by hole transfer between the VB of $FeTiO_3$ and TiO_2.

1. Introduction

Removal of environmental pollutants in water and air through photocatalytic reaction has attracted extensive interest over the last few decades [1–3]. Among various semiconductors, TiO_2 has been known as an excellent photocatalyst with its unique characteristics in band position and surface structure, as well as its extended chemical stability and nontoxicity [4–7]. Due to its large bandgap ($E_g = 3.2$ eV), however, TiO_2 can only utilize the photons in the UV region ($\lambda < 380$ nm), which limits its practical application in sun light or indoor [8–11]. One of the promising strategies to overcome this drawback is the coupling of TiO_2 with other narrow bandgap semiconductors capable of harvesting the photons in the visible range [12,13]. Many studies have reported on the sensitizer-loaded TiO_2 presenting photocatalytic activity under visible light irradiation, such as CdS/TiO_2, Cu_2O/TiO_2, $CdSe/TiO_2$, and others [14–28]. In most of these composites, the conduction band (CB) of the loaded sensitizer is located higher than that of TiO_2. Thus the electrons photogenerated by the sensitizer can be transferred to TiO_2 with visible light irradiation, and these transferred electrons on the CB of TiO_2 initiate various reduction reactions, as illustrated in Scheme 1a. However, such photoreduction reactions only lead to a partial decomposition of pollutants, and are difficult to induce CO_2 evolution. Moreover, the photogenerated holes remain on the valence band (VB) of the sensitizer, and the accumulation of holes on the sensitizer may lead to the photocorrosion of the catalyst and limit the repetitive use of the composite photocatalyst [29].

For the complete mineralization of contaminants and for the photochemical stability of catalyst, a new strategy utilizing the photogenerated holes will be necessary, and this may be achieved by designing the energy band of sensitizer in the TiO_2-based composite. That is, when the VB level of the sensitizer is lower than that of TiO_2, as illustrated in Scheme 1b, the electrons in the VB of TiO_2 will be transferred to that of the sensitizer, and the holes consequently generated in the VB of TiO_2 can be used for photooxidation reactions. This enables the complete decomposition of pollutants, considering the powerful oxidative ability of photogenerated holes. However, to the best of our knowledge, the concept of a heterojunction-type photocatalyst, utilizing the hole transfer between sensitizer and TiO_2, has not yet been realized. Herein we report the development of a $FeTiO_3/TiO_2$ heterojunction that induced complete decomposition of organic pollutants under visible light irradiation.

$FeTiO_3$, with a band gap of 2.58–2.9 eV [30–33], has been used as a chemical catalyst and photocatalyst [31,32]. Ye et al. observed that under UV irradiation the TiO_2–Fe_3O_4 mixed oxide coatings exhibited higher photocatalytic efficiency than the naked TiO_2 due

* Corresponding author. Tel.: +82 32 863 1026; fax: +82 32 867 5604.
E-mail address: wanin@inha.ac.kr (W.I. Lee).

0926-3373/$ – see front matter © 2008 Elsevier B.V.. All rights reserved.
doi:10.1016/j.apcatb.2008.02.017

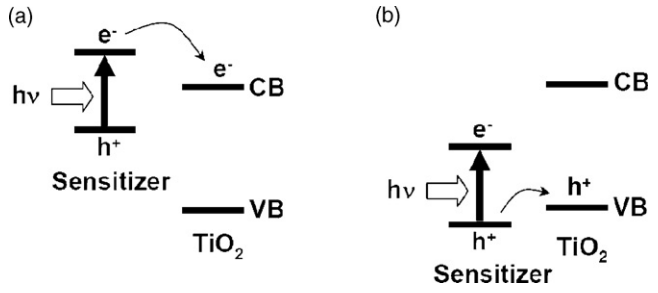

Scheme 1. Energy band diagram illustrating the coupling of TiO_2 with the narrow band-gap sensitizers, in which the charge carrier is transferred to the TiO_2 by visible light activation. (a) Electron transfer to CB of TiO_2 and (b) hole transfer to VB of TiO_2.

to the formation of $FeTiO_3$ [32,33], which may form a p–n junction with TiO_2, and may induce the spatial separation of the photogenerated electrons and holes. Although they suggested that the $FeTiO_3$ formation can extend the absorption wavelength to the visible region and thereby enhance the photocatalytic activity in the TiO_2–Fe_3O_4 mixed oxides, the detailed role of $FeTiO_3$ was not investigated. In the present study, the $FeTiO_3/TiO_2$ heterojunction was prepared by a simple sol–gel method, and applied to the photocatalytic degradation of 2-propanol in gas phase and 4-chlorophenol in aqueous solution under visible light irradiation. The mechanistic role of $FeTiO_3$ was discussed based on the photocatalytic behaviors of $FeTiO_3/TiO_2$ composites.

2. Experimental

2.1. Preparation of $FeTiO_3/TiO_2$ composites

One gram of $FeTiO_3$ particles (Aldrich) was dispersed and stirred in a mixed solution containing 50 ml of anhydrous ethanol, 1 ml of concentrated nitric acid, and 1.1 ml of deionized water. After vigorously stirring for 10 min, the stoichiometric amount of titanium isopropoxide (97%, Aldrich) was added slowly to this mixture. The as-obtained sol solution was gently stirred at ambient condition for 48 h to evaporate the solvent. The remained gel was dried at 100 °C for 12 h, and subsequently calcined at 450 °C for 1 h. As a blank experiment, the pure TiO_2 was prepared by the same procedure without $FeTiO_3$ addition.

2.2. Characterization

X-ray diffraction (XRD) patterns were obtained for the $FeTiO_3/TiO_2$ powder samples by using a Rigaku Multiflex diffractometer with monochromated high-intensity Cu Kα radiation. XRD scanning was performed under ambient conditions over the 2θ region of 15–80° at a rate of 2 °/min (40 kV, 20 mA). BET surface areas of the samples were measured with a surface area and porosimetry analyzer (UPA-150, Microtrac Inc.). UV–vis diffuse reflectance spectra were acquired by a PerkinElmer Lambda 40 spectrophotometer. $BaSO_4$ was used as the reflectance standard. Transmission electron microscope (TEM) images were obtained by a Philips CM30 operated at 250 kV. One milligram of $FeTiO_3/TiO_2$ was dispersed in 50 mL of methanol, and a drop of the suspension was then spread on a holey amorphous carbon film deposited on the copper grid.

The flat-band potentials (V_{fb}) of TiO_2 and $FeTiO_3$ were determined by electrochemical method [31]. Each of TiO_2 and $FeTiO_3$ particle was deposited as a film form on a 1 cm × 1 cm FTO glass. The V_{fb} was determined by extrapolation of a plot of the square of the photocurrent versus applied potential in 1 M KCl. Ag/AgCl and Pt were used as reference and counter electrode, respectively, and the irradiated light was monochromatic light of 330 nm.

2.3. Evaluation of photocatalytic activity

First, the prepared $FeTiO_3/TiO_2$ samples were tested as photocatalyst in decomposing 2-propanol in gas phase. An aqueous suspension containing 4.0 mg of $FeTiO_3/TiO_2$ (or other photocatalysts) was spread on a 2.5 cm × 2.5 cm Pyrex glass in a film form, which was subsequently dried at 50 °C for 2 h. The gas reactor system used for this photocatalytic reaction has been described elsewhere [34]. For the measurement of photocatalytic activity under visible light, the whole $FeTiO_3/TiO_2$ film area was irradiated by a 300 W Xe lamp through a UV cut-off filter (<420 nm, Oriel) and a water filter. After evacuating the reactor, 0.08 μL of 2-propanol mixed in 1.6 μL of water was added to the 200 mL gas-tight reactor. Then the initial concentration of gaseous 2-propanol in the reactor was kept to 117 ppm in volume (ppmv). Thus the ultimate concentration of CO_2 evolved will be 351 ppmv when the whole 2-propanol is completely decomposed, as shown in the following equation:

$$2(CH_3)_2CHOH\,(g) + 9O_2(g) \rightarrow 6CO_2\,(g) + 8H_2O\,(g)$$

The total pressure of the reactor was then controlled to 700 Torr by filling with oxygen gas. After a certain time of irradiation, 0.5 mL of the gas sample was automatically picked up from the reactor, and sent to a gas chromatograph (Agilent Technologies, Model 6890N). For the detection of CO_2, a methanizer was installed between the GC column outlet and the FID detector.

Second, for the degradation of 4-chlorophenol in aqueous solution, 50 mg of the $FeTiO_3/TiO_2$ composite was dispersed in 50 mL of 50 μM 4-chlorophenol aqueous solution by magnetic stirring. The remnant 4-chlorophenol after the irradiation of visible light was analyzed from its characteristic absorption peak detected by UV–vis spectrophotometer (PerkinElmer Lambda 40).

3. Results and discussion

TEM images of the 28 wt% $FeTiO_3$ and 72 wt% TiO_2 composite (28/72 $FeTiO_3/TiO_2$), as shown in Fig. 1a–c, indicate that the TiO_2 nanoparticles in the size of 10–20 nm are mutually aggregated and cover the surface of the 1–2-μm sized $FeTiO_3$ particles. The high-resolution TEM image in Fig. 1c suggests that a tight contact is formed between the TiO_2 nanoparticles and the large $FeTiO_3$ particles. Selected area electron diffraction (SAED) patterns were obtained for the TiO_2 region (inside of the dotted rectangular part in Fig. 1b). As shown in Fig. 1d, the well-defined ring patterns were identified as the characteristic diffraction patterns of the TiO_2 in the anatase phase, indicating that the coatings on the surface of $FeTiO_3$ consist of the pure polycrystalline anatase grains.

Fig. 2 shows the XRD patterns of the pure $FeTiO_3$, TiO_2 and $FeTiO_3/TiO_2$ composites with different compositions. The diffraction peaks at 24.04°, 32.74°, 35.41°, and 48.93°, as shown in Fig. 2a, correspond to the (0 1 2), (1 0 4), (1 1 0), and (0 2 4) peaks of the rhombohedral $FeTiO_3$ structure (JCPDS, No. 75-1211), respectively, whereas all of the diffraction peaks in Fig. 2g are identified as the pure anatase phase. The diffraction peaks in Fig. 2b–f indicate the $FeTiO_3/TiO_2$ composites to be a mixture of the rhombohedral $FeTiO_3$ and the anatase TiO_2 phases with no other impurity phases, suggesting that no appreciable chemical reaction occurred between TiO_2 and $FeTiO_3$ during the calcination at 450 °C.

BET surface area of pure $FeTiO_3$ was 3.1 m^2/g, whereas that of pure TiO_2 was 140 m^2/g. The surface area of $FeTiO_3/TiO_2$ composites increased gradually with increase of TiO_2 content (79/21 $FeTiO_3/TiO_2$: 32 m^2/g, 56/44 $FeTiO_3/TiO_2$: 69 m^2/g, 39/

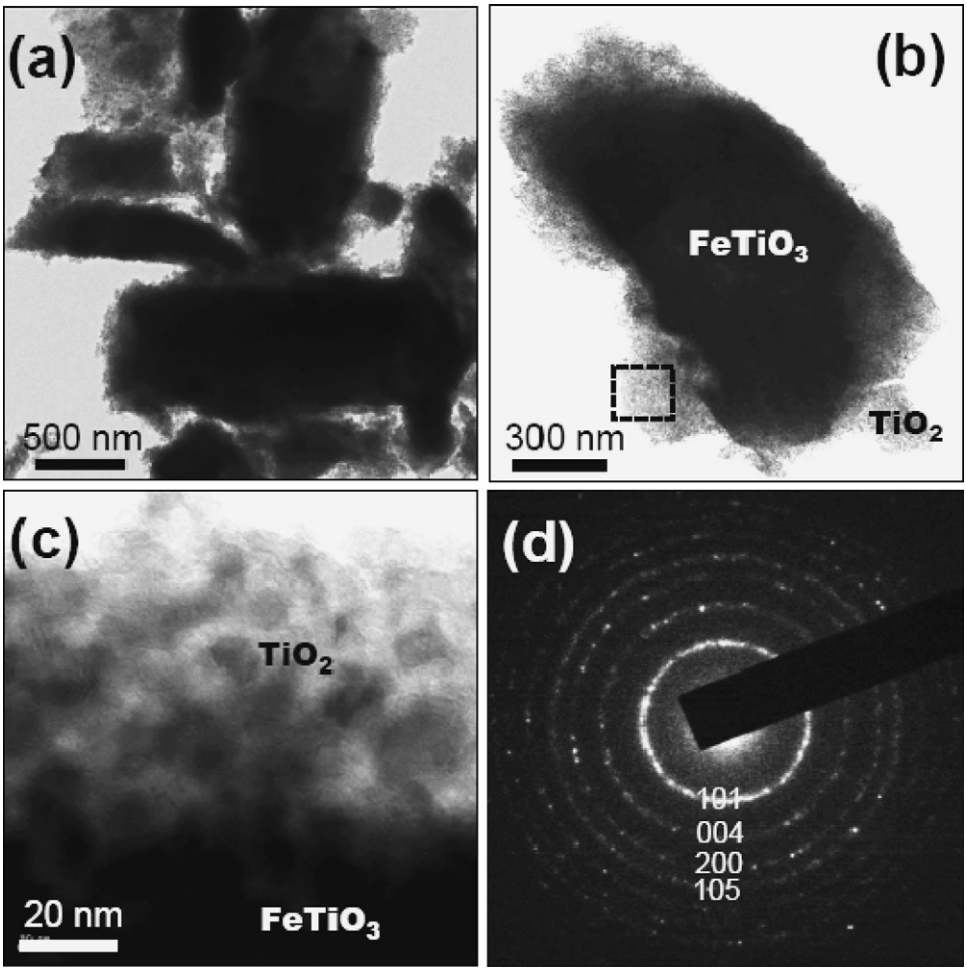

Fig. 1. (a and b) TEM images of the 28/72 $FeTiO_3/TiO_2$ composite, and (c) its high-resolution image. (d) SAED patterns for the TiO_2 nanoparticles (inside of the dotted rectangular part in (b)) coated on the $FeTiO_3$ surface.

61 $FeTiO_3/TiO_2$: 101 m^2/g, 28/72 $FeTiO_3/TiO_2$: 112 m^2/g, and 20/80 $FeTiO_3/TiO_2$: 121 m^2/g).

Fig. 3 shows UV–vis diffuse reflectance spectra for the pure TiO_2, $FeTiO_3$ and $FeTiO_3/TiO_2$ composites. Due to its wide band gap, TiO_2 showed a high reflectance in visible region, whereas $FeTiO_3$ revealed a notably strong absorption in the whole solar spectrum. Hence, the $FeTiO_3/TiO_2$ composites exhibited significantly high absorption in the visible region, which was further enhanced with increasing $FeTiO_3$ content. Although the bandgap of $FeTiO_3$ was reported to be about 2.58–2.9 eV [35,36], no characteristic peak

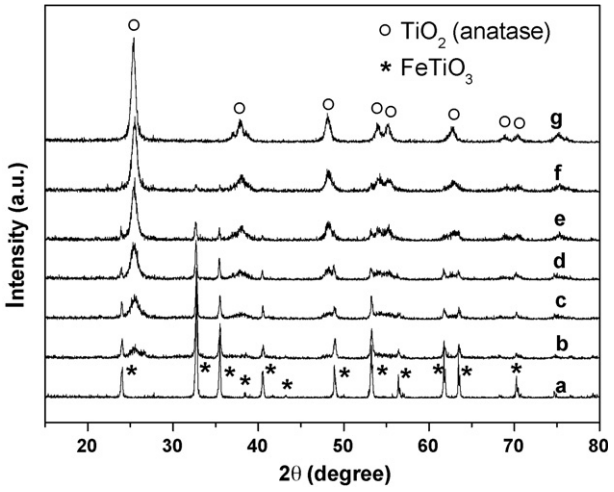

Fig. 2. XRD patterns of TiO_2, $FeTiO_3$ and $FeTiO_3/TiO_2$ composites at different compositions: (a) $FeTiO_3$, (b) 79/21 $FeTiO_3/TiO_2$, (c) 56/44 $FeTiO_3/TiO_2$, (d) 39/61 $FeTiO_3/TiO_2$, (e) 28/72 $FeTiO_3/TiO_2$, (f) 20/80 $FeTiO_3/TiO_2$, and (g) TiO_2.

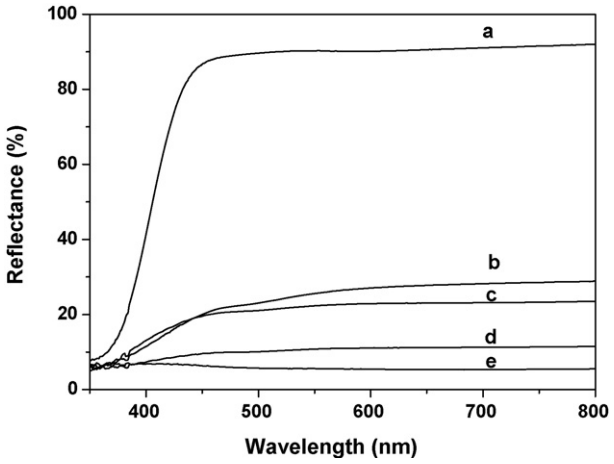

Fig. 3. UV–vis diffuse reflectance spectra of TiO_2, $FeTiO_3$ and the $FeTiO_3/TiO_2$ composites: (a) TiO_2, (b) 20/80 $FeTiO_3/TiO_2$, (c) 28/72 $FeTiO_3/TiO_2$, (d) 56/44 $FeTiO_3/TiO_2$, and (e) $FeTiO_3$.

due to the band gap excitation of $FeTiO_3$ was observed in the diffuse reflectance spectra of the pure $FeTiO_3$ and the $FeTiO_3/TiO_2$ composites. This phenomenon was caused by the intervalence charge transfer between Fe^{2+} and Ti^{4+} ($Fe^{2+} + Ti^{4+} \rightarrow Fe^{3+} + Ti^{3+}$) in $FeTiO_3$ [36]. The strong absorption of the $FeTiO_3/TiO_2$ composites in the visible region implies efficient utilization of visible light for the photocatalytic reaction.

The photocatalytic activities of the $FeTiO_3/TiO_2$ composites in decomposing 2-propanol in gas phase were evaluated under a visible light irradiation ($\lambda \geq 420$ nm). As shown in Fig. 4a, the photocatalytic activities of pure TiO_2, Degussa P25 and $FeTiO_3$ were very low under visible light irradiation. By contrast, the $FeTiO_3/TiO_2$ composites in several compositions showed notably high photocatalytic activity under visible light irradiation. Especially, the 28/72 $FeTiO_3/TiO_2$ exhibits the highest activity. That is, about 16% of 2-propanol was decomposed in 2 h irradiation. At $FeTiO_3$ content exceeding 28 wt%, the photocatalytic activity of the composites was gradually decreased.

The photocatalytic activity was also evaluated according to the amount of CO_2 evolved during the visible light irradiation. As shown in Fig. 4b, the $FeTiO_3/TiO_2$ composites in several compositions demonstrated notably high photocatalytic activity, whereas both the pure TiO_2 and $FeTiO_3$ showed very low efficiency. The highest photocatalytic activity was observed from the 28/72 $FeTiO_3/TiO_2$ composite: the evolved CO_2 was 8.2 ppmv after 2 h irradiation. Its efficiency generating CO_2 was more than three times of that of Degussa P25. The great increase of CO_2 evolution demonstrates that the visible-light-irradiated $FeTiO_3/TiO_2$ composite can induce complete mineralization of 2-propanol without formation of intermediate species caused by partial decomposition.

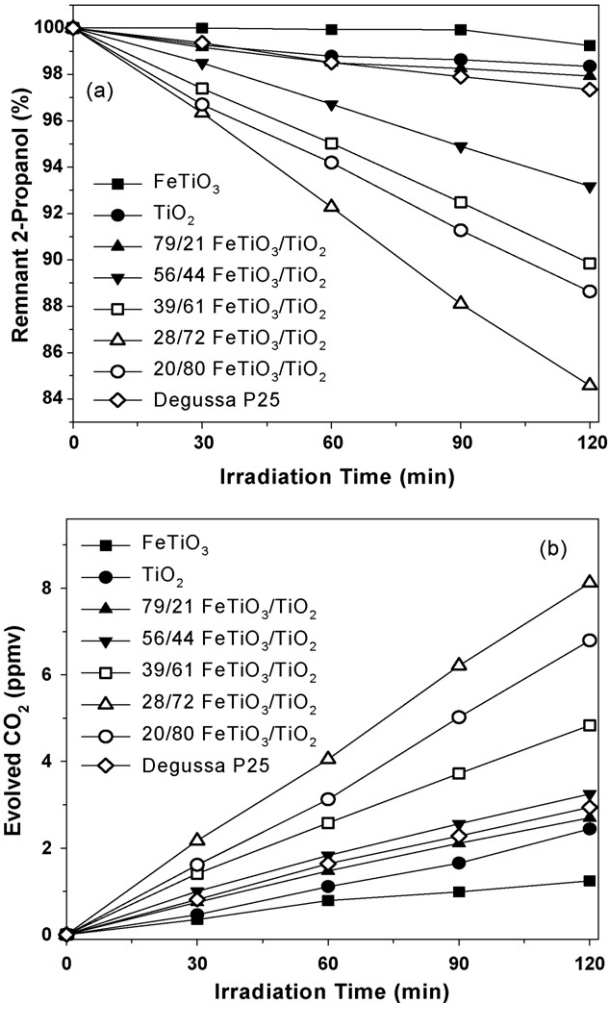

Fig. 4. Photocatalytic decomposition of gaseous 2-propanol as a function of irradiation time. (a) Percentage of remnant 2-propanol and (b) amount of CO_2 evolved.

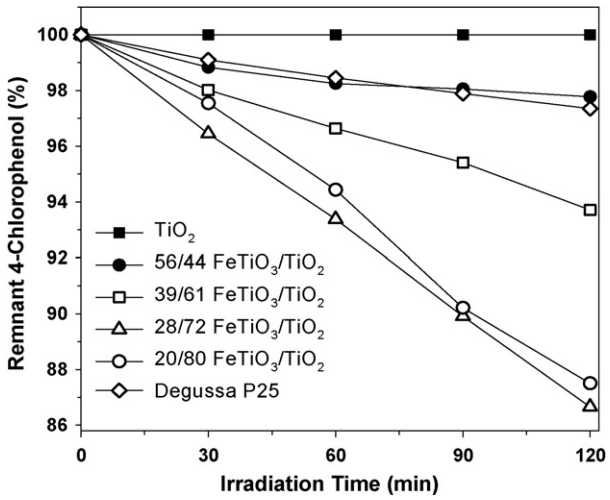

Fig. 5. Photocatalytic degradation of 4-chlorophenol in aqueous suspension of TiO_2, Degussa P25, and several $FeTiO_3/TiO_2$ composites as a function of irradiation time.

The photocatalytic activity of $FeTiO_3/TiO_2$ was also evaluated according to the removal of 4-chlorophenol dissolved in aqueous solution. The remnant 4-chlorophenol after the irradiation of visible light was analyzed from its characteristic absorption peak detected by UV–vis spectroscopy. Fig. 5 indicates the degradation rates of 4-chlorophenol with several $FeTiO_3/TiO_2$, TiO_2, and P25 samples. The observed photocatalytic activity trends for the reactions in aqueous solution were similar to those in gas phase. The 28/72 $FeTiO_3/TiO_2$ showed the highest photocatalytic activity, by decomposing 13% of 4-chlorophenol after 2 h irradiation.

To test the photochemical stability, the 28/72 $FeTiO_3/TiO_2$ sample was retrieved and reused three times for the photocatalytic reaction in aqueous solution. After each photocatalytic reaction, the $FeTiO_3/TiO_2$ in aqueous solution was collected and dried at 100 °C for repeated use. As shown in Fig. 6, the recycled $FeTiO_3/TiO_2$ does not show any appreciable change in photocatalytic activity, which emphasizes the chemical stability of the composite photocatalyst.

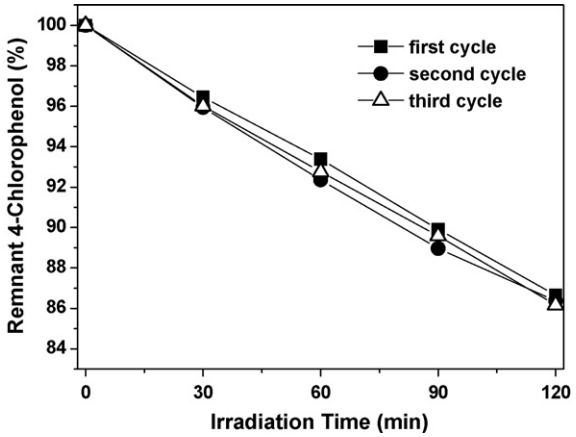

Fig. 6. Cyclic photodegradation of aqueous 4-chlorophenol under visible light irradiation by repeated use of the 28/72 $FeTiO_3/TiO_2$ composite.

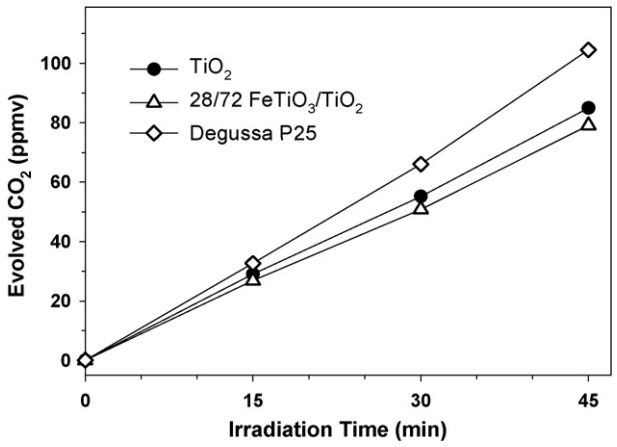

Fig. 7. Rate of CO_2 evolution from the photocatalytic decomposition of 2-propanol under irradiation of mixed UV and visible light. A 300 W Xe lamp without UV cut-off filter was used as light source.

The photocatalytic activities of the 28/72 $FeTiO_3/TiO_2$ samples were also evaluated under a mixture of UV and visible light (A 300 W Xe lamp without applying the UV cut-off filter was used as light source.). As shown in Fig. 7, the 28/72 $FeTiO_3/TiO_2$ does not show higher photocatalytic activity than pure TiO_2 or P25. This suggests that the photocatalytic activity of TiO_2 under UV region is not appreciably affected by the heterojunction with $FeTiO_3$.

Coupling of TiO_2 with other semiconductors has been frequently investigated to improve the photocatalytic activity of TiO_2 in order to promote the separation of photogenerated charge carriers and/or to extend the absorption wavelength up to the visible region. In the present study, both TiO_2 and $FeTiO_3$ showed a very low photocatalytic activity under a visible light irradiation, but their heterojunction demonstrated notably high activity. It is deduced that the unusually high efficiency of the $FeTiO_3/TiO_2$ composite originates from the unique relative band positions of these two semiconductors. Herein, the relative band positions of TiO_2 and $FeTiO_3$ were determined by an electrochemical method [31]. The flat-band potentials (V_{fb}) of these semiconductors were obtained by extrapolation of a plot of the square of the photocurrent versus applied potential. The differences of V_{fb} between these semiconductors would be more

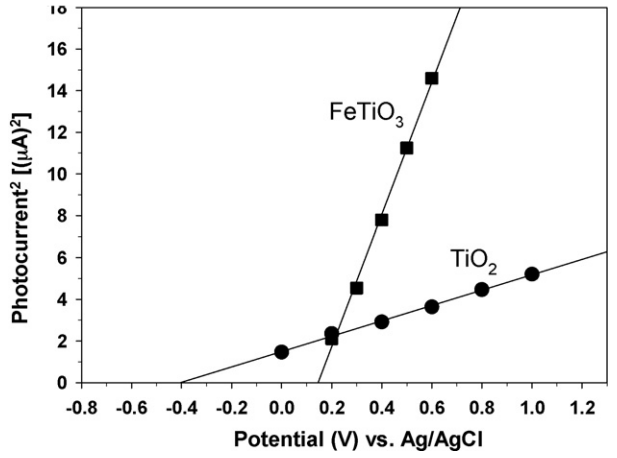

Fig. 8. The square of the photocurrent vs. applied potential in 1 M KCl for TiO_2 (anatase) and $FeTiO_3$. Ag/AgCl and Pt were used as reference and counter electrode, respectively, and the irradiated light was monochromatic light of 330 nm.

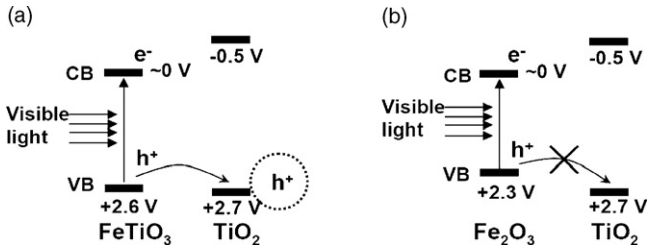

Fig. 9. Proposed mechanism for the visible light photocatalytic activity of (a) $FeTiO_3/TiO_2$ and (b) Fe_2O_3/TiO_2.

reliable data than the absolute energy levels, since the V_{fb} is critically dependent on pH. It has been found from the plots in Fig. 8 that V_{fb} position of $FeTiO_3$ is lower than that of TiO_2 by 0.53 V. Since the CB position of TiO_2 is known as −0.5 V (vs. NHE), that of $FeTiO_3$ is estimated to ~0 V (vs. NHE). Wilson et al. theoretically calculated the energy band of $FeTiO_3$ [36]. They indicated that in the $FeTiO_3$ structure the position of the O 2p states is largely unaffected and thus the upper valence band is dominated by O 2p character. That is, the Fe 3d–O 2p hybridization is reduced to zero leaving a small Ti 3d contribution to the almost pure O 2p character of the valence band. This implies that VB position of $FeTiO_3$ is very close to that of TiO_2 (−2.7 V vs. NHE), which is compatible with our experimental result determined by electrochemical method. Furthermore, the VB position of $FeTiO_3$ obtained in this work is coincident with other reported values, calculated based on the electronegativity of the constituent atoms [32,33,37,38].

As indicated in Fig. 9a, the electrons in the VB of $FeTiO_3$ can be excited to its CB with visible light irradiation. Thereby, the VB of $FeTiO_3$ is rendered partially vacant, and the electrons in the VB of TiO_2 can be transferred to that of $FeTiO_3$, since the VB positions of these semiconductors are not appreciably different. As a result, the holes generated in the VB of TiO_2 have sufficient lifetime to initiate the photocatalytic oxidation reactions. By this inter-semiconductor hole-transfer mechanism, the photogenerated charge carriers can be separated efficiently so that the composite can utilize the visible light to degrade pollutants. In addition, $FeTiO_3$ has extraordinary high absorption over the entire visible light range. This is unique and notable advantage of $FeTiO_3$ as a visible-light-sensitizer, since a large quantity of electron and hole pairs can possibly be generated by the efficient absorption of visible light.

In order to test this hole-transfer mechanism, α-Fe_2O_3 instead of $FeTiO_3$ was introduced for the formation of the composite with TiO_2. The band gap of α-Fe_2O_3 in the corundum phase is 2.3 eV [39–41], which is close to that of $FeTiO_3$. However, an essential difference between Fe_2O_3 and $FeTiO_3$ is the position of the energy band. That is, the VB of Fe_2O_3 (+2.3 V) is appreciably higher than that of $FeTiO_3$ (+2.6 V) [40,41]. Hence, as shown in Fig. 9b, the VB of Fe_2O_3 is considerably higher than that of TiO_2, and the transfer of holes from the VB of Fe_2O_3 to that of TiO_2 would be difficult as a result.

The preparation condition of the Fe_2O_3/TiO_2 composites was the same as that of $FeTiO_3/TiO_2$. As the relative compositions between Fe_2O_3 and TiO_2 were varied from 0:100 to 100:0, the photocatalytic activity under the visible light was monotonously decreased. That is, as shown in Fig. 10, the 28/72 Fe_2O_3/TiO_2 did not show improved photocatalytic activity compared to the pure TiO_2 in the degradation of 2-propanol under visible light irradiation, whereas the 28/72 $FeTiO_3/TiO_2$ demonstrated a great enhancement. We believe that the difference in photocatalytic behavior between these two systems is closely related to the

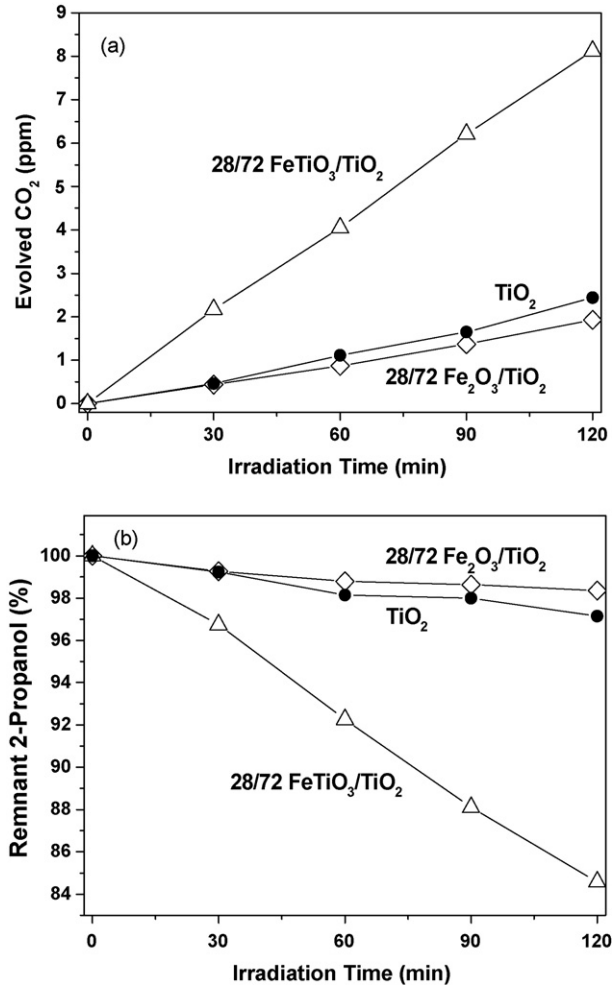

Fig. 10. Comparison of the photocatalytic activity of $FeTiO_3/TiO_2$ and Fe_2O_3/TiO_2 under visible light irradiation ($\lambda \geq 420$ nm). (a) Percentage of remnant 2-propanol and (b) amount of CO_2 evolved.

relative VB position between the sensitizer semiconductor and TiO_2. This could be an example supporting the hole-transfer mechanism occurring at the $FeTiO_3/TiO_2$ heterojunction. Further investigation on this system is continuing in our laboratory, and more attention is necessary for this heterojunction-type photocatalyst working under visible light.

4. Conclusions

A new photocatalyst was formed from the heterojunction between various compositions of $FeTiO_3$ and TiO_2. The 28/72 $FeTiO_3/TiO_2$ composite exhibited a notably high photocatalytic activity in the complete decomposition of organic compounds under visible light irradiation. The high efficiency of the $FeTiO_3/TiO_2$ composite was considered to be caused by the unique relative band positions of these two semiconductors and the profound absorption of visible light by $FeTiO_3$. The close VB position of $FeTiO_3$ (+2.6 V) to that of TiO_2 (+2.7 V) enabled the hole transfer from the VB of $FeTiO_3$ to that of TiO_2. Therefore, the visible light absorption by $FeTiO_3$ induced the generation of holes on TiO_2, which resulted in the complete decomposition of the organic compounds.

Acknowledgments

The authors gratefully acknowledge the financial support of the Ministry of Environment, Republic of Korea (Project No. 022-061-026), and the Ministry of Information and Communication of Korea under the ITRC support program (IITA-2008-C109008010030).

References

[1] M.R. Hoffmann, S.T. Martin, W. Choi, D.W. Bahnemann, Chem. Rev. 95 (1995) 69.
[2] E.S. Tang, J.H. Won, S.J. Hwang, J.H. Choy, Adv. Mater. 18 (2006) 3309.
[3] H. Luo, T. Takata, Y. Lee, J. Zhao, K. Domen, Y. Yan, Chem. Mater. 16 (2004) 846.
[4] Z. Ding, G.Q. Lu, P.F. Greenfield, J. Phys. Chem. B 104 (2000) 4815.
[5] Y. Huang, Z. Zheng, Z. Ai, L. Zhang, X. Fan, Z. Zou, J. Phys. Chem. B 110 (2006) 19323.
[6] J.C. Yu, J. Yu, W. Ho, Z. Jiang, L. Zhang, Chem. Mater. 14 (2002) 3808.
[7] Y. Ou, J. Lin, S. Fang, D. Liao, Catal. Commun. 8 (2007) 936.
[8] S. Sakthivel, H. Kisch, ChemPhysChem 4 (2003) 487.
[9] W. Zhao, W. Ma, C. Chen, J. Zhao, Z. Shuai, J. Am. Chem. Soc. 126 (2004) 13574.
[10] R. Asahi, T. Morikawa, T. Ohwaki, K. Aoki, Y. Taga, Science 293 (2001) 269.
[11] S. Klosek, D. Raftery, J. Phys. Chem. B 105 (2001) 2815.
[12] W. Ho, J.C. Yu, J. Lin, J. Yu, P. Li, Langmuir 20 (2004) 5865.
[13] S.Y. Chai, Y.J. Kim, W.I. Lee, J. Electroceram. 17 (2006) 909.
[14] Y. Bessekhouad, N. Chaoui, M. Trzpit, N. Ghazzal, D. Robert, J.V. Weber, J. Photochem. Photobiol. A 183 (2006) 218.
[15] W. Ho, J.C. Yu, J. Mol. Catal. A: Chem. 247 (2006) 268.
[16] H. Song, H. Jiang, X. Liu, G. Meng, J. Photochem. Photobiol. A 181 (2006) 421.
[17] B. Pal, M. Sharon, G. Nogami, Mater. Chem. Phys. 59 (1999) 254.
[18] H. Yin, Y. Wada, T. Kitamura, T. Sakata, H. Mori, S. Yanagida, Chem. Lett. 30 (2001) 334.
[19] A. Kumar, A. Jain, J. Mol. Catal. A: Chem. 165 (2001) 265.
[20] Y. Bessekhouad, D. Robert, J.V. Weber, J. Photochem. Photobiol. A 163 (2004) 569.
[21] S.C. Lo, C.F. Lin, C.H. Wu, P.H. Hsieh, J. Hazard. Mater. 114 (2004) 183.
[22] J. Liu, R. Yang, S. Li, Rare Met. 25 (2006) 636.
[23] X. Yu, Q. Wu, S. Jiang, Y. Guo, Mater. Charact. 57 (2006) 333.
[24] J.S. Jang, S.M. Ji, S.W. Bae, H.C. Son, J.S. Lee, J. Photochem. Photobiol. A 188 (2007) 112.
[25] L. Ge, M. Xu, H. Fang, J. Mol. Catal. A: Chem. 258 (2006) 68.
[26] J.C. Tristão, F. Magalhães, P. Corio, M.C. Sansiviero, J. Photochem. Photobiol. A 181 (2006) 152.
[27] J.S. Jang, W. Li, S.H. Oh, J.S. Lee, Chem. Phys. Lett. 425 (2006) 278.
[28] M.G. Kang, H.E. Han, K.J. Kim, J. Photochem. Photobiol. A 125 (1999) 119.
[29] N. Serpone, P. Maruhamuthu, P. Pichat, E. Pelizzetti, H. Hidaka, J. Photochem. Photobiol. A 85 (1995) 247.
[30] X. Tang, K. Hu, J. Mater. Sci. 41 (2006) 8025.
[31] D.S. Ginley, M.A. Butler, J. Appl. Phys. 48 (1977) 2019.
[32] F. Ye, A. Ohmori, C. Li, Surf. Coat. Technol. 184 (2004) 233.
[33] F. Ye, A. Ohmori, Surf. Coat. Technol. 160 (2002) 62.
[34] Y.T. Kwon, K.Y. Song, W.I. Lee, G.J. Choi, Y.R. Do, J. Catal. 191 (2000) 192.
[35] Z. Dai, H. Naramoto, K. Narumi, J. Appl. Phys. 85 (1999) 7433.
[36] N.C. Wilson, J. Muscat, D. Mkhonto, P.E. Ngoepe, N.M. Harrison, Phys. Rev. B 71 (2005) 075202.
[37] H. Zhang, S. Ouyang, Z. Li, L. Liu, T. Yu, J. Ye, Z. Zou, J. Phys. Chem. Solids 67 (2006) 2501.
[38] Y. Xu, M. Schoonen, Am. Miner. 85 (2000) 543.
[39] W. Wang, F. Huang, X. Lin, Scr. Mater. 56 (2007) 669.
[40] F. Chen, Y. Xie, J. Zhao, G. Lu, Chemosphere 44 (2001) 1159.
[41] C. Damm, R. Herrmann, G. Israel, F.W. Müller, Dyes Pigm. 74 (2007) 335.